Superhydrophobicity on transparent fluorinated ethylene propylene films with nano-protrusion morphology by Ar+O_2 plasma etching: Study of the degradation in hydrophobicity after exposure to the environment

Nitant Gupta,[1] M. V. Kavya,[1] Yogesh R. G. Singh,[1] J. Jyothi,[1] and Harish C. Barshilia[1, a)]

Surface Engineering Division, CSIR-National Aerospace Laboratories, Post Bag No. 1779, Bangalore 560 017, India

Fluorinated ethylene propylene (FEP) films were made superhydrophobic by Ar+O_2 plasma etching process. Field emission scanning electron microscopy and atomic force microscopy studies of the plasma-treated FEP samples detected the presence of uniformly distributed nano-protrusions exhibiting a low surface roughness necessary for maintaining the transparency of the samples. In fact, optical transmittance measurements showed an improvement in the transparency of FEP samples after plasma treatment. The X-ray photoelectron spectroscopic analysis showed the presence of $-CF_x-O-CF_x-$ (x=1, 2 or 3) linkages in both untreated and plasma-treated samples which explains the hydrophilic nature (contact angle below 90°) of the untreated sample. Fourier transform infrared spectroscopy showed no changes in the bulk properties of the plasma-treated samples. Moreover, exposure to the environment caused the surfaces to lose their superhydrophobic property in an indefinite amount of time. This has been further studied through a water immersion experiment and explained through the wetting state transition from Cassie state to Wenzel state.

Keywords: Fluorinated Ethylene Propylene Films, Superhydrophobicity, Ar+O_2 Plasma Etching Process, Nano-protrusion Morphology

a)Author for correspondence:

E-mail address: harish@nal.res.in; Fax # +91-80-2521 0113; Tel. # +91-80-2508 6494

I. INTRODUCTION

Superhydrophobicity is the surface phenomenon that represents extreme water repellency. Superhydrophobic surfaces are known to exhibit very high static water contact angles (above 150°) and very low roll-off angles.[1] Presence of uniformly distributed micro/nano-scale features on a surface can render a surface superhydrophobic provided that the surface has a low surface free energy (SFE). This condition results in the reduction of the contact angle hysteresis (defined as the difference between the advancing and the receding contact angles) which controls pinning of water droplets to the surface, and hence controls droplet mobility.

The behavior of a droplet on a smooth surface was first characterized by Thomas Young in 1805.[2] Young's equation gives the balance of surface energies between the three interfacial energies corresponding to the solid-vapor (γ_{sv}), solid-liquid (γ_{sl}) and liquid-vapor (γ_{lv}) interfaces and also, relates them to the contact angle (θ) of the smooth surface. This relationship is given as:

$$\cos\theta = \frac{\gamma_{sv} - \gamma_{sl}}{\gamma_{lv}}. \tag{1}$$

Surface of a low SFE material is a hydrophobic surface as it exhibits a water contact angle of more than 90° which tells us that the water adhesion is less ($\gamma_{sv} < \gamma_{sl}$). On the other hand, surfaces of high SFE materials have a lower than 90° water contact angle (more adhesion; $\gamma_{sv} > \gamma_{sl}$), and are therefore termed as hydrophilic surfaces. For rough surfaces, the theories put forward by Wenzel[3] and Cassie-Baxter[4] are widely used in explaining their wetting phenomenon. According to Wenzel's theory,[3] by increasing the roughness of a surface, the nature of water affinity of the surface magnifies, i.e., the surface becomes more hydrophobic or hydrophilic, depending on it being initially hydrophobic or hydrophilic, respectively. However, Wenzel's theory is only applicable for uniformly rough surfaces which are in the total wetting regime. More often, the Cassie state of wetting exists, where partial wetting of the surface occurs. This is possible if substantial amount of air cavities reside under the droplet of water as per Cassie-Baxter's theory.[4] This state is responsible for the superhydrophobic property of most surfaces. A droplet in the Cassie state is highly mobile and can easily roll-off the surface which is a characteristic of superhydrophobic phenomenon.

Surfaces with high surface energy can also sustain Cassie wetting state and exhibit superhydrophobicity. However, transitions in the wetting state occur when these surfaces are

exposed to water (or humid environment) for long durations. Eventually, these surfaces lose their droplet mobility and pinning of water droplets occurs due to complete transition to Wenzel wetting state. This phenomenon was observed by us previously for the case of superhydrophobic Mg alloy samples,[5] and is now observed in the present study (discussed later).

Various techniques involving surface modifications have been used to develop superhydrophobic surfaces over the past 15 years, and many different materials have been made superhydrophobic as a result of one or more of these methods.[6–14] Plasma etching of polymeric substrates is an effective treatment for fabrication of superhydrophobic surfaces, as it involves utilization of highly reactive plasma species to modify the functionality of the substrate.[15] In the past we have used $Ar+O_2$ plasma to prepare superhydrophobic Kapton® and Polytetrafluoroethylene (PTFE) surfaces.[16,17] Here we describe our results on the plasma treatment of fluorinated ethylene propylene(FEP) fluoropolymer. It is well-known that fluoropolymers usually have low SFE due to the presence of strong C-F bonds, and thus, their surfaces can be easily manipulated to make them superhydrophobic, as has also been done by us in the past.[17–19]

FEP is a copolymer of tetrafluoroethylene (CF_2=CF_2) and hexafluoropropylene (CF_2=$CF-CF_3$). It is a linear, semicrystalline fluoroplastic and has properties similar to other fluoropolymers like Polytetrafluoroethylene (PTFE). Its structure is represented as:

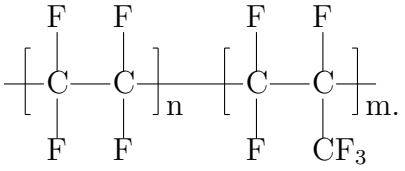

The crystallinity of FEP is less because its chain packing is only 70% (compared to 98% of PTFE) due to the presence of fluoromethyl groups in the fluoroalkane chains[20]. FEP is chemically inert, can withstand extreme temperature conditions, has low friction and antistiction properties, has excellent optical and electrical properties, and is easily processable using conventional thermoplastic methods[21]. FEP is commercially available as a transparent film which can be heat sealed, thermoformed, welded and heat bonded[22]. It is currently used in various research applications related to aerospace and biomedical fields[23–26].

In the present work, we have developed superhydrophobic FEP surfaces that also retain their transparency. This is made possible because the observed superhydrophobic behaviour

does not require a microscale roughness. The nanoscale roughness, thus present, is too less to scatter visible light, which helps in sustaining the transparency of the FEP samples. However, it was observed that exposure to the environment for long durations causes these samples to lose their droplet mobility, and eventually the superhydrophobic behavior degrades to hydrophilic behavior. We have studied this phenomenon and provided a plausible explanation which may cause it to happen. We also tried to stabilize the superhydrophobic behaviour of our FEP samples by depositing a silane coating, which is a very popular technique.[27] We believe that these surfaces will have widespread applications in various optical devices and also may lead to novel innovations in aerospace and biomedical fields.

II. EXPERIMENTAL DETAILS

Fig. 1 gives an overview of the plasma etching process used to generate superhydrophobic FEP surfaces. DuPont™ Teflon® FEP films (type: C-20, thickness: 125 μm) were cut into 40 mm square pieces, and cleaned with isopropyl alcohol, through ultrasonic agitation for 10 min. Surface treatments were carried out in a plasma reactor, the details of which are given in an earlier paper.[28] A pulsed bias power supply (Huttinger, PBP-3) was used to create Ar+O_2 plasma. The operating pressure for the plasma treatment was maintained at 15 mTorr (2 Pa). The plasma current and power varied as 65-175 mA and 25-130 W, respectively. The temperature of the sample during plasma treatment was measured using a chromel-alumel thermocouple. The different parameters used to create the plasma and to control the surface morphology of FEP were, (a) the substrate temperature, (b) the gas flow rate of O_2, (c) the substrate negative bias voltage (applied to the substrate holder; hereafter referred to as the substrate voltage), and (d) the duration of plasma etching (or treatment time). Variation of surface properties was measured by changing one parameter and keeping the other parameters constant. Initial parameters were determined by trial to get the superhydrophobic property, and were 150 °C, 18 sccm, 600 V and 60 min, respectively. All the parameters were varied below and above their initial values. Substrate temperature was varied as 30 (room temperature), 100, 150 and 200°C. The O_2 gas flow rate was varied from 10 to 26 sccm at 4 sccm intervals, while the Ar flow rate was maintained at 28 sccm. Substrate voltage was varied from 400 to 750 V at 50 V intervals. Finally, the duration of plasma treatment was varied from 15 to 90 min at 15 min intervals. All the results obtained

after characterization studies of the samples were found to be reproducible (the error range observed in the static contact angle was within $\pm 2^{\circ}$) and hence, it can be said that the plasma etching process shows good repeatability.

Since the samples were heated during plasma etching, it was observed that while keeping the substrate (as it is) on the holder, it would usually stick to the substrate plate, and was needed to be peeled out. This also caused partial loss in its transparency. Therefore, the samples were loaded in the vacuum chamber by keeping square slotted metal plates, (shown in Fig. 1), above and below the FEP sample. This enabled the substrate to be suspended in free space (with no contact from any side), and resulted in an etched area of 20 mm x 20 mm (area of interest). The area of interest remained transparent, demonstrated superhydrophobic property, and was used for all the characterization studies.

Plasma-treated FEP samples were characterized using static contact angle measurements, atomic force microscopy (AFM), field emission scanning electron microscopy (FESEM), X-ray photoelectron spectroscopy (XPS), optical transmittance measurements and fourier transform infrared spectroscopy (FTIR). Static water contact angles were measured by the sessile drop method using a Phoenix-300 plus contact angle goniometer (Surface Electro Optics). Three separate regions of the same sample were used to measure the contact angles and their average values were reported. The morphology of the untreated and plasma treated samples were studied using FESEM (Supra 40VP, Carl Zeiss). Since the samples were non-conducting, a gold sputtered thin film was deposited on their surfaces prior to FESEM measurements. The average surface roughness of the FEP samples was calculated using AFM measurements. Surfaces of the samples were scanned at three different regions and the average roughness was calculated for each to check the consistency in the results. Optical transmittance measurements were made from UV-VIS-NIR Lambda 750 spectrophotometer (Perkin-Elmer). Detailed chemical analysis of the surface layer was performed by XPS using SpecsLab2 (Version 2.57-r18860) with achromatic Al Kα radiation (1486.6 eV) operated at 12 kV and 12.5 mA X-ray source. The binding energies reported here were referenced to C 1s peak at 285 eV. FTIR spectra was obtained by Spectrum GX FTIR spectrometer (Perkin-Elmer).

III. RESULTS AND DISCUSSION

A. Parameter optimization of Ar+O_2 plasma etching process

Static contact angle measurements are one of the most popular ways to characterize the superhydrophobicity of a surface and hence, they were used to optimize the parameters that controlled the Ar+O_2 plasma characteristics. The process described here was found to be repeatable to an error of $\pm 2^\circ$ in the contact angle values. It may be noted, that the untreated samples demonstrated a contact angle of 84°. Fig. 2 shows the dependence of contact angles to the Ar+O_2 plasma etching process parameters, such as, the substrate temperature, the flow rate of O_2, the substrate voltage and the duration of plasma etching, as discussed below:

1. Substrate temperature

In Fig. 2(a) the contact angle is plotted with respect to the substrate temperature, as the substrate was heated at constant temperature during the plasma etching process. The other parameters were maintained at their initial values (18 sccm, 600 V and 60 min). The contact angle of the sample at room temperature (about 30 °C) was 149°. As the temperature was increased, the samples showed improvement in the contact angle values demonstrating 156° at 100 °C, 157° at 150 °C, and 156° at 200 °C. Thus, it can be said that the heating of the substrate during plasma etching favored the induction of superhydrophobic property. 150 °C was chosen as the optimum temperature for further experiments.

2. O_2 flow rate

Fig. 2(b) illustrates the variation in contact angle with the O_2 flow rate. The substrate temperature was maintained at the optimum value (150 °C) and other parameters were kept at their initial values (600 V, 60 min). The contact angles at flow rates of 10, 14, 18, 22 and 26 sccm were found to be 152°, 153°, 155°, 153° and 154°, respectively. However, it was observed that at lower O_2 flow rates (10 and 14 sccm) the superhydrophobic property was not uniformly distributed. Apart from this, the O_2 flow rate did not seem to affect the properties of the FEP sample, and hence, might not be getting directly incorporated on the

FEP surface. The value of 18 sccm was chosen as the optimum O_2 flow rate.

3. Substrate voltage

Keeping the temperature and O_2 flow rate at their optimum values (150 °C, 18 sccm), the substrate voltage was varied from 400 to 750 V. The changes in the contact angle are plotted in Fig. 2, and are found to vary in a narrow range of 155°-157°. Since the error in repeatability is 2°, all the samples exhibit about the same contact angle with substrate voltage variation. However, as seen from Fig. 3(a), the surface roughness of these same samples changes with the substrate voltage. The average surface roughness (R_a) of plasma-treated FEP surfaces at the substrate voltages (Fig. 3(a)) in the range of 400 to 550 V increased from 14 to 29 nm while for higher substrate voltages (600-750 V), it stayed in the range of 40 nm. FESEM and AFM profiles of these samples in Fig. 4 give further information about the surface morphology of these samples. Fig. 4(a) gives the smooth profile of the untreated FEP sample showing a surface roughness of 8.1 nm. While, in Fig. 4(b) (450 V), 4(c) (550 V) and 4(d) (650 V) the nano-protrusions formed as a result of the plasma etching process seem to have less variation in the lateral dimensions (average distance between the protrusions appears to be the same). So the variation in roughness is due to changes in the maximum height of the protrusions, given as 0.25, 0.26 and 0.35 μm, respectively.

Since the surface roughness of the plasma-treated FEP samples varies significantly with the substrate voltage, the changes in the optical transmittance intensity as a result can also be observed in Fig. 5. A significant observation here is that the transmittance intensity of the untreated sample (curve (a)) is less than that of the sample treated at 400 and 450 V (curves (b) and (c)), for the entire wavelength range (350-800 nm).The reason behind this is attributed to the application of heat during plasma treatment process. To confirm this, an untreated FEP sample was vacuum annealed, in the same plasma reactor, for 60 min at 150 °C. The inset in Fig. 5 shows that the vacuum annealed sample also shows improvement in the optical transmittance characteristics, as compared to the untreated sample. At substrate voltages of 500, 550 and 600 V, the optical transmittance improves after around 420 nm wavelength (curves (d), (e) and (f)). For samples treated at higher substrate voltages (650 and 700 V in curves (g) and (h)), the optical transmittance is lesser

than the untreated sample till about 700 nm wavelength. The optical transmittance of the 750 V sample is markedly less than the untreated sample (curve (i)). These variations in optical transmittance intensity are in good agreement with the surface roughness variations that were observed in Fig. 3(a). It was also observed that the samples with lower substrate voltage (or lower surface roughness) lost their superhydrophobic behavior earlier than the samples with higher substrate voltage (or higher surface roughness) after being exposed to the environment (more details are given in the next subsection).

4. Treatment time

Since superhydrophobic nature was already demonstrated at each substrate voltage value, the variation for the time duration of plasma etching was carried out at 450 V, as its optical transmittance was found to be superior to all the other FEP samples. Fig. 2(d) gives the contact angle variation with treatment time at 450 V. It is observed that there is a systematic increase in the contact angle with the treatment time. The contact angle of the untreated FEP sample was 84° which indicates a slightly hydrophilic nature. However, the plasma-treated samples etched for 15, 30, 45, 60, 75 and 90 min exhibited contact angles as 142°, 150°, 151°, 156°, 156° and 157°, respectively. Correspondingly, the plot in Fig. 3(b) shows a gradual increase in the surface roughness from 14 to 25 nm for treatment times 15-90 min. These samples also show similar surface profiles as seen from the FESEM and AFM measurements in Fig. 6. The feature sizes for these samples are similar and the observed variation in height of protrusions is also less. Thus, it might be concluded, that the effect of substrate voltage was more profound than the plasma etching time, in determining the characteristics of nano-protrusions, in terms of their feature size and density.

B. Wettability of the plasma-treated FEP samples and effects of environmental exposure

To have a closer look at the plasma-treated FEP surface, a high resolution FESEM micrograph was taken for the FEP sample at 600 V (substrate voltage) and 60 min (treatment time) as shown in Fig. 7(a). The micrograph shows a more detailed structure (shape and size) of the nano-protrusions that are present on the surface. The formation of protrusion

is a well-known phenomenon on fluorinated polymers like PTFE and FEP after plasma treatment.[17,29–31] However, the protrusions observed in the case of Ar+O_2 plasma-treated FEP samples are in the nanoscale, i.e., they are thinner, smaller and denser than the protrusions reported in other reports.[29–31] The mechanism of protrusion formation has been discussed by Kitamura et al.[30,31] for the case of PTFE and FEP samples (by ion beam irradiation), and their analyses state that for the case of FEP the protrusion formation is more advanced, dense and uniformly distributed. The nanoscale roughness due to the presence of nano-protrusions is the main reason that the plasma-treated FEP samples retain their transparency, since surface roughness and transparency are inversely proportional to each other. Nanoscale roughness of the order of 40 nm is not sufficient to scatter visible light.[32]

Fig. 7(b) is a schematic representation of the wetting state of the superhydrophobic FEP samples. As can be seen the water droplet resides strictly on the top of the nano-protrusions, representing the Cassie state wetting. Since the surface energy of the plasma-treated FEP sample is high, water makes a concave surface in between two protrusions. This enables the water droplet to change its wetting state from Cassie state to Wenzel state when the water droplet is in contact with the surface for long durations. This is what causes the surface to lose its superhydrophobic nature when exposed to the environment. However, the time taken to make the transition (varies from hours to weeks) depends upon the surface roughness of the sample. In our case, the samples treated at different substrate voltages initially showed almost the same contact angle. But it was observed that the samples with lower substrate voltage (lower roughness) lost their superhydrophobicity earlier than the samples with higher substrate voltage (higher roughness).

The samples were further examined by XPS and FTIR spectroscopy to study the chemical changes as a result of the plasma treatment. The chemical nature of the surface layer of plasma-treated FEP samples was analyzed by XPS. Apart from analyzing the results for the untreated and the plasma-treated FEP samples, we have also included the XPS scans of the plasma-treated samples that were exposed to the environment for longer durations and had lost their superhydrophobic property. The environmentally exposed sample has been referred to as the degraded sample. The elemental XPS survey scan in the range of 0 to 1100 eV, for the untreated, plasma-treated and degraded FEP samples, detected the presence of carbon (C 1s), oxygen (O 1s) and fluorine (F 1s) elements as shown in Fig. 8. The high reduction in the fluorine peak intensity as compared to the carbon peak in

the plasma-treated and the degraded sample demonstrates that these samples have higher crosslinking.[33] It is also important to note that the presence of oxygen in the untreated FEP sample is higher (in intensity) than usually reported.[34,35] This may have raised the surface energy of the untreated sample and is responsible for the hydrophilic contact angle of the untreated FEP sample (84°) as opposed to 109° which has been reported in literature[35]. To understand the detailed stoichiometry of the surface layer, core level spectra of C 1s and O 1s for the plasma-treated FEP samples were also obtained.

The deconvoluted peaks for the carbon (C 1s) spectra, in Fig. 9, reveal the presence of $-C-C-$ (285 eV), $-C-CF_x-$ (286-287 eV), $>CF-O-CF_2-$ (291 eV), $>CF-$ (290 eV), $-CF_2-$ (291 eV), $-CF_3$ (293 eV) and $-CF_2-O-CF_2-$ (294 eV) bonding species along with other possible variants[33,34,36,37]. The individual peak assignment in this case seems to be ambiguous and some peaks may have contributions from more than one species. The changes in the peak intensities in the second envelope (envelope E2 in Fig. 9) indicates that the chain structure of the surface changes after the plasma treatment which also substantiates cross-linking.[33,38] Due to the defluorination of the plasma treated samples, probably in the form of CF_4 gas,[20] the intensity of the $-CF_3$ peak (294 eV) declined (envelope E1). The presence of $>CF-O-CF_2-$ and $-CF_2-O-CF_2-$ linkages is detected in the untreated FEP samples itself. The intensities corresponding to these peaks seem to have decreased after the plasma treatment, which suggests that oxygen may not have been incorporated into the chain from the $Ar+O_2$ plasma. The decrease in the intensity for the $-CF_x-O-CF_x-$ ($x =$ 1 or 2, sometimes 3) species can also be seen from the core level spectra of the O 1s in Fig. 10. The peaks corresponding to oxygen in $>CF-O-CF_2-$ and $-CF_2-O-CF_2-$ are at binding energies of 534 and 535-536 eV (envelope E3), respectively.[34,37] Thus, the oxygen atoms are present in between the chain in the form of $-CF_x-O-CF_x-$ linkages and may have caused the high surface energy of the FEP samples.

FTIR studies (Fig. 11) were also performed on the untreated (curve a), plasma-treated (curve b) and the degraded (curve c) samples to compare the chemical nature of the bulk FEP substrate. The very strong band between 1100 and 1300 cm^{-1} corresponds to the stretching modes of $-CF_2-$.[29,33] The peak at 980 cm^{-1} belongs to $-CF_3$ linkages.[29,33] The minor peaks in the range of 1400 to 2000 cm^{-1} can be attributed to the crosslinking groups.[29,33] As can be observed clearly the spectra of the three samples appear to be identical, indicating no changes to the bulk material as a result of the plasma treatment.

We have previously mentioned that the plasma-treated samples were losing their superhydrophobicity after exposure to the environment for long durations. It was also observed that frequent contact with water resulted in an earlier loss of the superhydrophobic property. To understand this phenomenon, a superhydrophobic sample (600 V, 60 min) was immersed in water for about 5 days. During this immersion experiment, the sample was taken out after certain intervals of time to measure its contact angle and then it was placed back into the water. The results of the immersion experiment are plotted in Fig. 12. It can be seen that after only 2 h immersion in water the contact angle drops from 157° to 97°. After 3 h immersion the contact angle becomes 73° which indicates that the sample now exhibits hydrophilic nature. Subsequent immersions resulted in further deterioration of the contact angle which ultimately dropped to about 37° after 120 h. We have said earlier, that the deterioration in the contact angle is caused due to the wetting state transitions that occur after getting exposed to the environment. This has been illustrated in Fig. 13 based on the observations made by the immersion experiment. Since the surface energy of the plasma-treated sample is high, it attracts the water into the nano-protrusions. As a result the water seeps into the nano-protrusions and replaces the air cavity. Since in Wenzel wetting state the apparent surface energy of the sample increases for a hydrophilic surface, the final contact angle (37°) exhibited by the plasma-treated FEP surface after environmental exposure is found to be much lower than 89°. The effect of immersion may have been to increase the apparent SFE of the plasma-treated FEP surface, possibly due to formation of $-$OH bondings on the surface.

In order to counter the effect of high surface energy of the FEP surface, as the cause for degradation in superhydrophobicity, we recommend silane treatment of the plasma-treated FEP samples. A monolayer of silane when coated on top of the FEP surface will mimic its roughness and also reduce the apparent SFE of the sample. Our trials with perfluorooctylsilane and vinyltrichlorosilane showed better retentivity of the superhydrophobic behavior, with marginal loss in transparency. However, with the right silane we believe that this can be further optimized. Characterization studies were not carried out on the silane-coated samples as they lie outside the scope of our present work.

IV. CONCLUSION

Transparent superhydrophobic FEP samples were prepared by Ar+O_2 plasma etching process. The substrate temperature was optimized at 150 °C and O_2 flow rate at 18 sccm. The samples demonstrated superhydrophobicity at all the substrate voltages and were found to have nano-protrusion morphology which imparted nanoscale roughness of the order of 10-50 nm. The maximum water contact angle obtained was 157°. The optical transmittance of sample with 450 V substrate voltage was found to higher than the untreated sample. The samples were found to have high SFE because of the presence of $-CF_x-O-CF_x-$ linkages in both untreated and plasma-treated FEP. The degradation in the superhydrophobicity was understood by a water immersion experiment, which demonstrated that wetting state transitions from Cassie to Wenzel state resulted in the decrease of the contact angle. It is proposed that with an optimized silane coating the apparent SFE of plasma-treated FEP surfaces can be lowered, without much loss of transparency, and the superhydrophobicity shall be retained for longer durations.

ACKNOWLEDGMENTS

The authors thank the director of CSIR-National Aerospace Laboratories, Bangalore for granting permission to publish these results. Mr. Praveen Kumar, Mr. Siju and Mr. Manikandananth are thanked for their assistance in characterization studies of FEP samples.

REFERENCES

[1]L. Feng, S. Li, Y. Li, H. Li, L. Zhang, J. Zhai, Y. Song, B. Liu, L. Jiang, and D. Zhu, Advanced Materials **14**, 1857 (2002).

[2]T. Young, Philosophical Transactions of the Royal Society of London **95**, 65 (1805).

[3]R. N. Wenzel, Industrial and Engineering Chemistry **28**, 988 (1936).

[4]A. B. D. Cassie and S. Baxter, Transactions of the Faraday Society **40**, 546 (1944).

[5]N. Gupta, S. Sasikala, and H. C. Barshilia, Nanoscience and Nanotechnology Letters **4**, 757 (2013).

[6]H. C. Barshilia, K. R. S. Tej, L. M. Devi, and K. S. Rajam, Journal of Applied Physics **108**, 074315 (2010).

[7]A. Chaudhary and H. C. Barshilia, The Journal of Physical Chemistry C **115**, 18213 (2011).

[8]H. C. Barshilia, N. Selvakumar, N. Pillai, L. M. Devi, and K. S. Rajam, Applied Surface Science **257**, 4410 (2011).

[9]H. C. Barshilia, S. John, and V. Mahajan, Solar Energy Materials and Solar Cells **107**, 219 (2012).

[10]P. Roach, N. J. Shirtcliffe, and M. I. Newton, Soft Matter **4**, 224 (2008).

[11]J. Fan and Y. Zhao, Langmuir **26**, 8245 (2010).

[12]W. J. Khudhayer, R. Sharma, and T. Karabacak, Nanotechnology **20**, 275302 (2009).

[13]M. Ma and R. M. Hill, Current Opinion in Colloid and Interface Science **11**, 193 (2006).

[14]X. Zhang, F. Shi, J. Niu, Y. Jiang, and Z. Wang, Journal of Materials Chemistry **18**, 621 (2008).

[15]R. Jafari, S. Asadollahi, and M. Farzaneh, Plasma Chemistry and Plasma Process **33**, 177 (2013).

[16]H. C. Barshilia, A. Ananth, N. Gupta, and C. Anandan, Applied Surface Science **268**, 464 (2013).

[17]H. C. Barshilia and N. Gupta, Vacuum **99**, 65 (2014).

[18]H. C. Barshilia, D. K. Mohan, N. Selvakumar, and K. S. Rajam, Applied Physics Letters **95**, 033116 (2009).

[19]N. Selvakumar, H. C. Barshilia, and K. S. Rajam, Journal of Applied Physics **108**, 013505 (2010).

[20]J. S. Forsythe and D. J. T. Hill, Progress in Polymer Science **25**, 101 (2000).

[21]"DuPont™ FEP Film-Information Bulletin," Tech. Rep. H-55007-3.

[22]"DuPont™ FEP Film-Properties Bulletin," Tech. Rep. H-55008-3.

[23]J. A. Dever, K. K. de Groh, B. A. Banks, J. A. Townsend, J. L. Barth, S. Thomson, T. Gregory, and W. Savagek, High Performance Polymers **12**, 125 (2000).

[24]J. P. Ranieri, R. Bellamkonda, J. Jacob, T. G. Vargo, J. A. Gardella, and P. Aebischer, Journal of Biomedical Materials Research **27**, 917 (1993).

[25]J. P. Ranieri, R. Bellamkonda, E. J. Bekos, T. G. Vargo, J. A. Gardella, and P. Aebischer, Journal of Biomedical Materials Research **29**, 779 (1995).

[26]F. Fanelli, G. Orgera, M. Bezzi, P. Rossi, M. Allegritti, and R. Passariello, European Radiology **18**, 911 (2008).

[27]L. Zhai, F. C. Cebeci, R. E. Cohen, and M. F. Rubner, Nano Letters **4**, 1349 (2004).

[28]H. Barshilia, K. Yogesh, and K. Rajam, Vacuum **83**, 427 (2009).

[29]A. Kitamura, T. Koboyashi, T. Satoh, M. Koka, T. Kamiya, A. Suzuki, and T. Terai, Nuclear Instruments and Methods in Physics Research B **307**, 614 (2013).

[30]A. Kitamura, T. Koboyashi, A. Suzuki, and T. Terai, Surface and Coatings Technology **206**, 841 (2011).

[31]A. Kitamura, T. Koboyashi, T. Meguro, A. Suzuki, and T. Terai, Surface and Coatings Technology **203**, 2406 (2009).

[32]A. Nakajima, K. Hashimoto, and T. Watanabe, Monatshefte fr Chemie / Chemical Monthly **132**, 31 (2001).

[33]S. Agraharam, D. W. Hess, P. A. Kohl, and S. A. B. Allen, Journal of Vacuum Science and Technology A **17**, 3265 (1999).

[34]B. Parekh, S. Zheng, A. Entenberg, T. Debies, and G. Takacs, Journal of Adhesion Science and Technology **21**, 983 (2007).

[35]H. J. Busscher, I. Stokroos, H. C. V. der Mei, P. G. Rouxhet, and J. M. Schakenraad, Journal of Adhesion Science and Technology **6**, 347 (1992).

[36]A. Tressaud, E. Durand, and C. Labrugére, Journal of Fluorine Chemistry **125**, 1639 (2004).

[37]W. Dasilva, A. Entenberg, B. Kahn, T. Debies, and G. A. Takacs, Journal of Adhesion Science and Technology **18**, 1465 (2004).

[38]B. J. Lyons, Radiation Physics Chemistry **45**, 159 (1995).

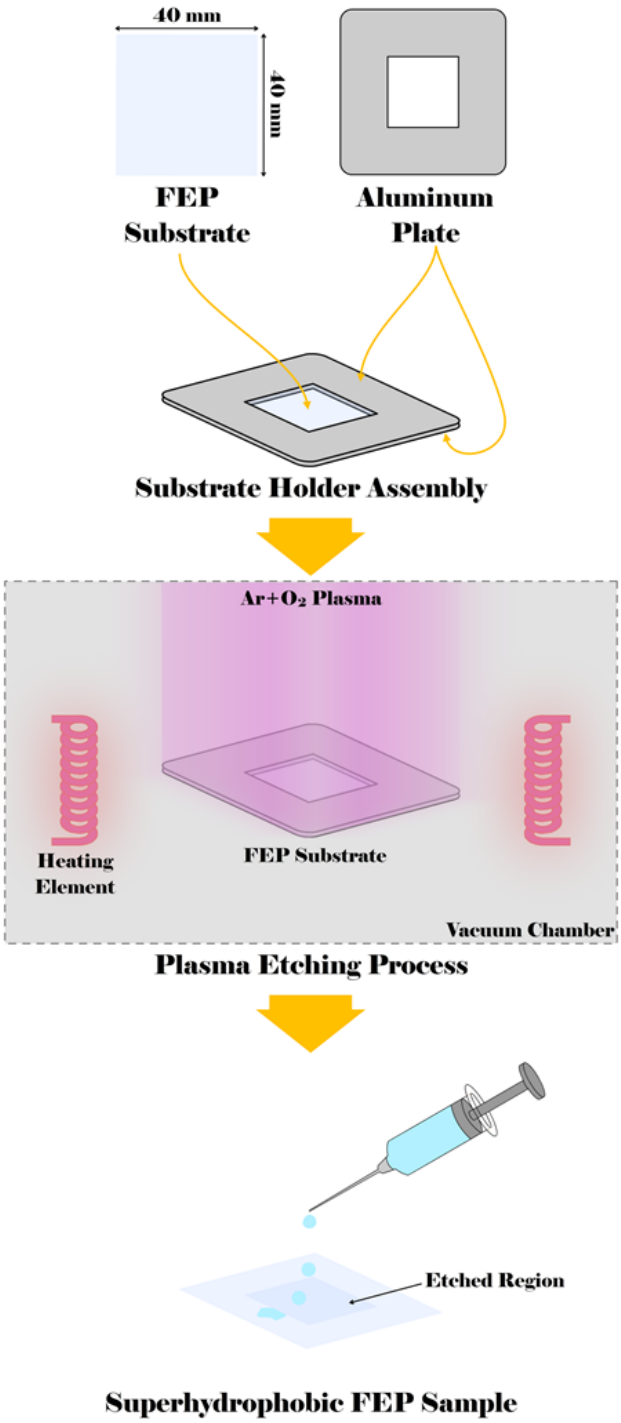

FIG. 1. Schematic of the plasma etching process for the production of superhydrophobic FEP samples.

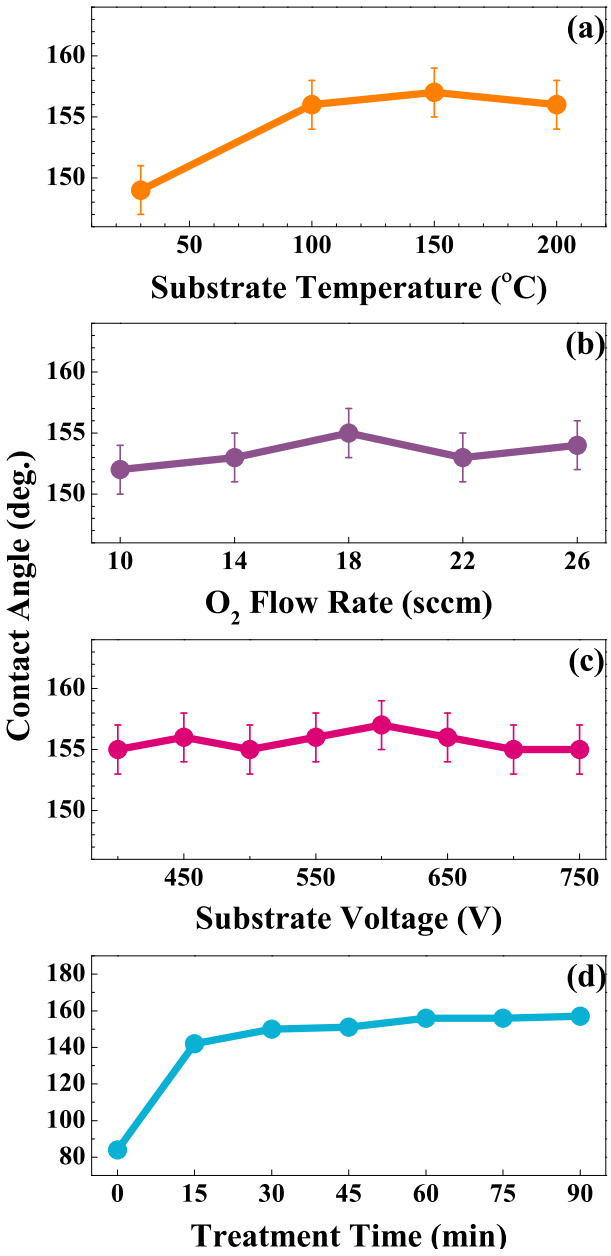

FIG. 2. Variation in the contact angle of FEP samples with different parameters used to control the Ar+O_2 plasma etching process: (a) substrate temperature, (b) O_2 flow rate, (c) substrate voltage and (d) plasma etching duration.

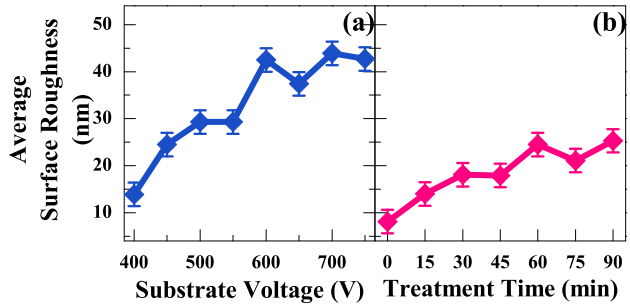

FIG. 3. Plot showing the change in the average surface roughness of FEP samples for (a) different substrate voltages and (b) different etching time durations.

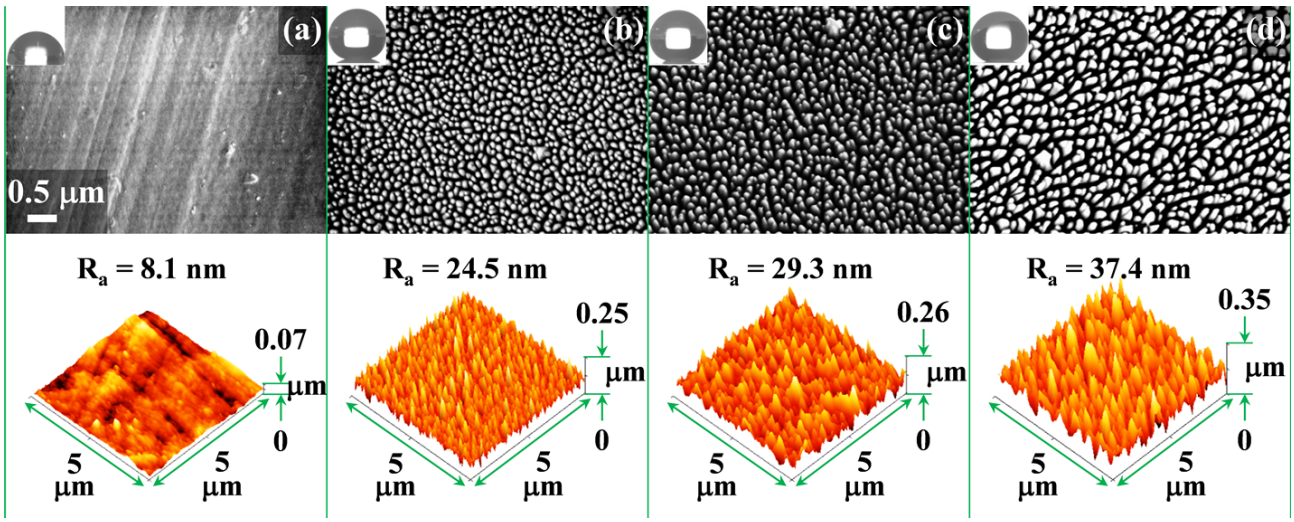

FIG. 4. FESEM micrographs and AFM surface profiles of FEP samples plasma etched for 60 min at (a) 0 V (untreated sample), (b) 450 V, (c) 550 V and (d) 650 V. The scale bar is same for all the FESEM micrographs. Insets provide the contact angle photograph of the corresponding samples. AFM profiles are drawn to the same scale for comparison.

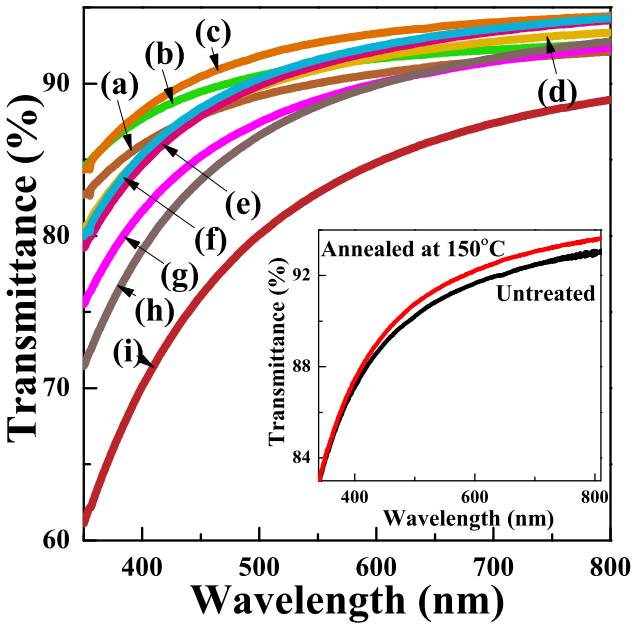

FIG. 5. Plot showing the optical transmittance intensity for the sample with different substrate voltages: (a) 0 (untreated), (b) 400, (c) 450, (d) 500, (e) 550, (f) 600, (g) 650, (h) 700 and (i) 750 V. The plot in the inset gives the comparison of the transmittance intensity between an annealed FEP sample (at 150 °C) and an untreated FEP sample.

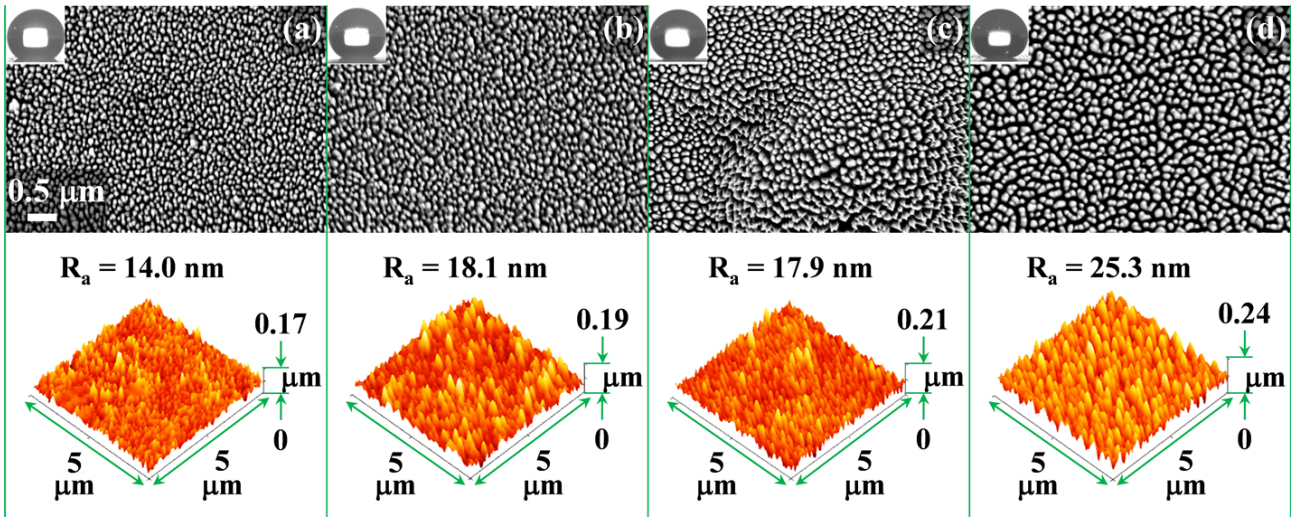

FIG. 6. FESEM micrographs and AFM surface profiles of FEP samples plasma etched at 450 V for (a) 15 min, (b) 30 min, (c) 45 min and (d) 90 min. The scale bar is same for all the FESEM micrographs. Insets provide the contact angle photograph of the corresponding samples. AFM profiles are drawn to the same scale for comparison.

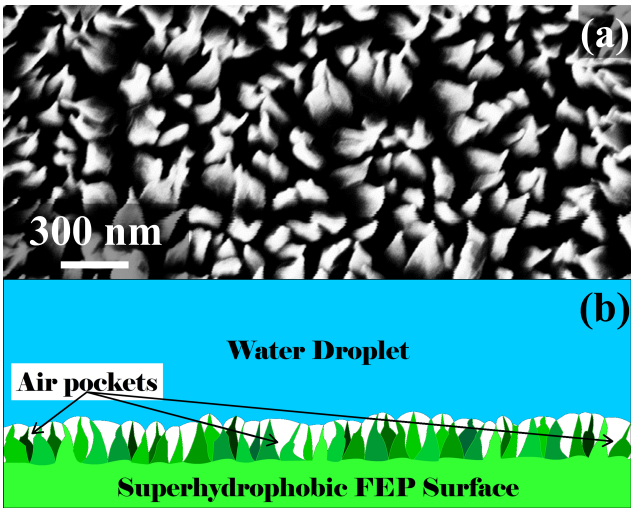

FIG. 7. (a) Higher resolution FESEM micrograph showing the shape of the nano-protrusions in detail. (b) Schematic representation of the water droplet in Cassie state on top of the nano-protrusions.

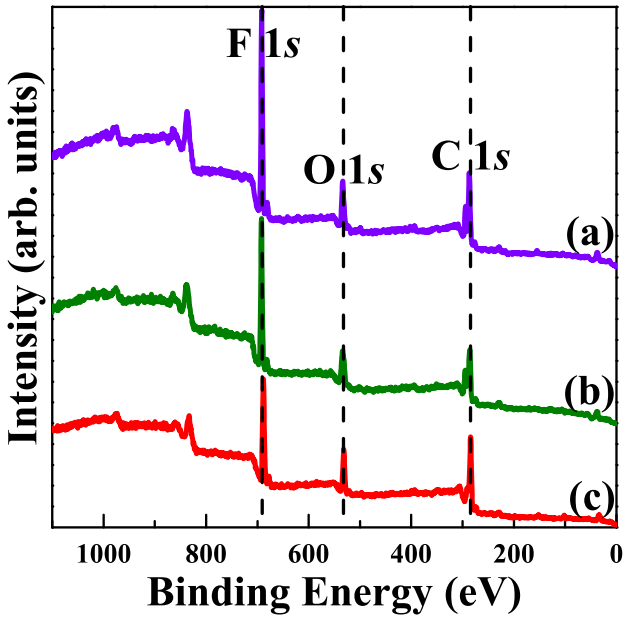

FIG. 8. XPS survey scan indicating the presence of Carbon, Fluorine and Oxygen in the (a) untreated, (b) plasma-treated, and (c) degraded (exposed to the environment for longer durations) FEP samples.

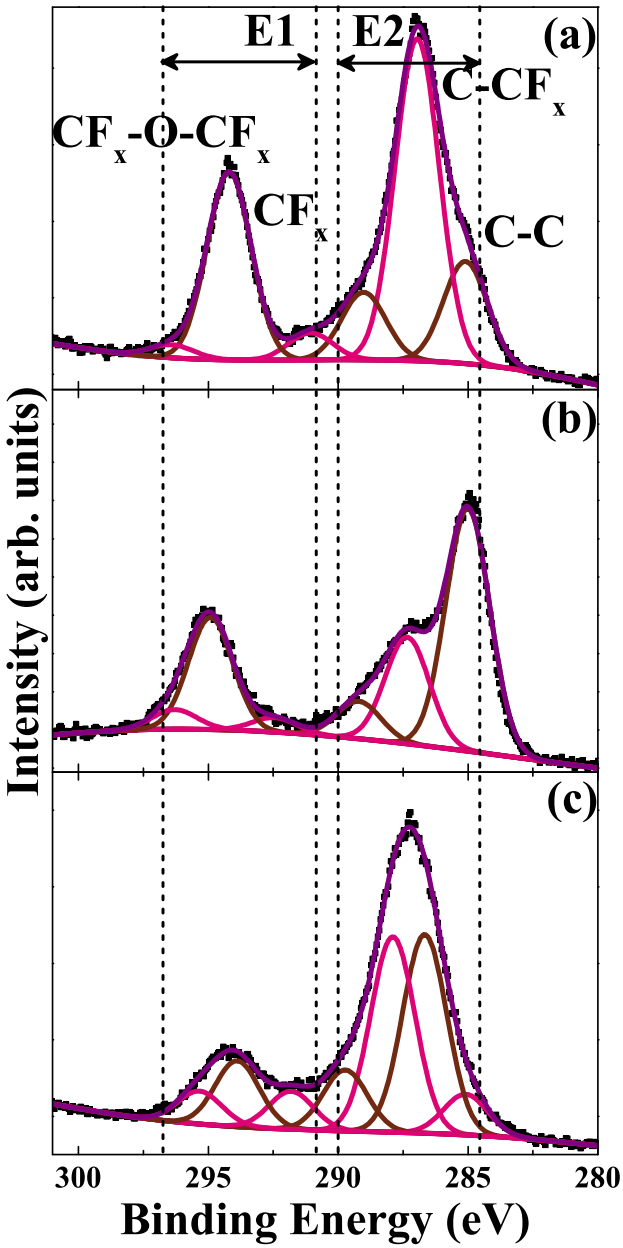

FIG. 9. XPS core level spectra of (a) untreated, (b) plasma-treated, and (c) degraded FEP samples for C 1s species.

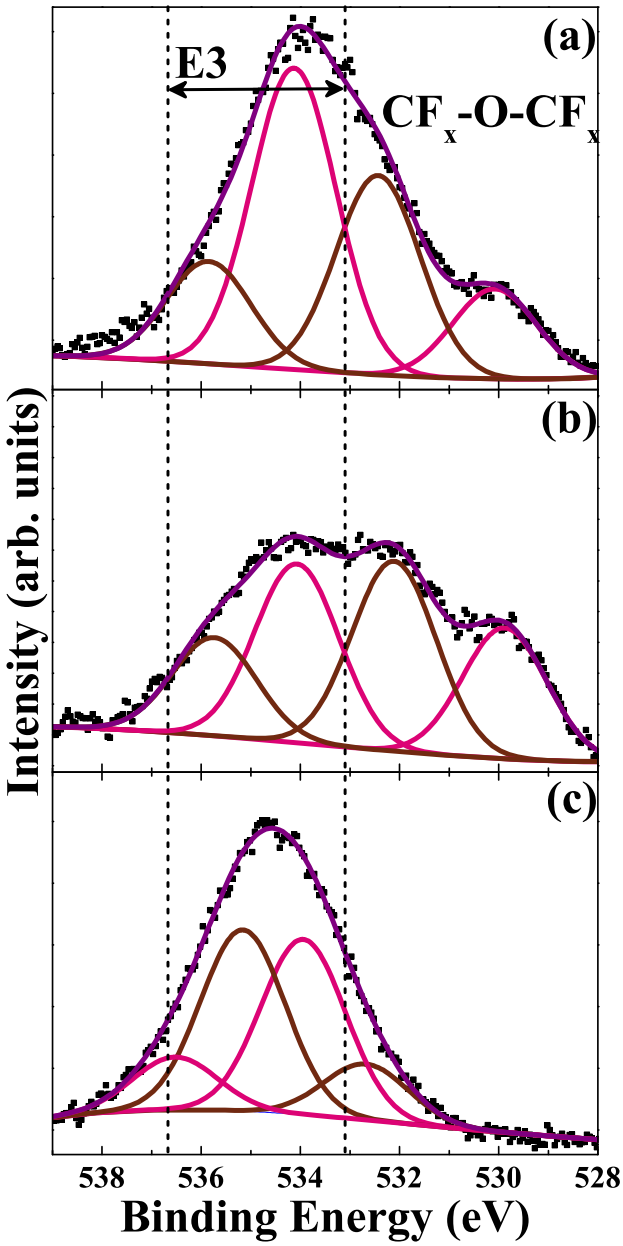

FIG. 10. XPS core level spectra of (a) untreated, (b) plasma-treated, and (c) degraded FEP samples for O 1s species.

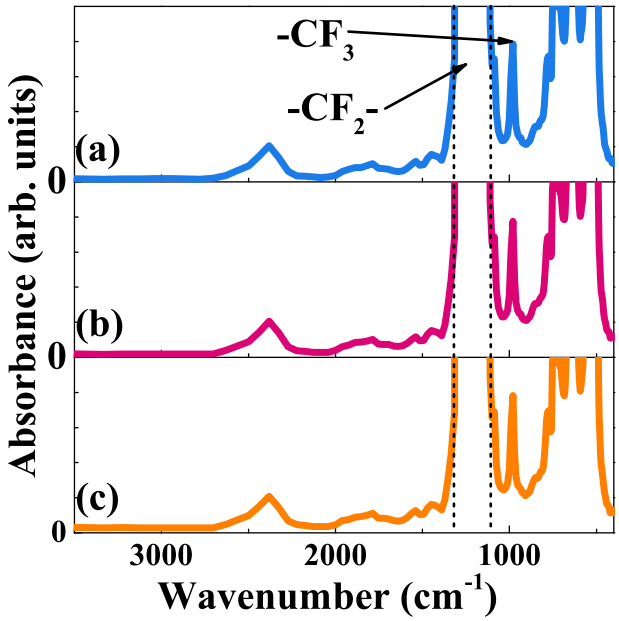

FIG. 11. FTIR spectra for the (a) untreated, (b) plasma-treated, and (c) degraded FEP surfaces.

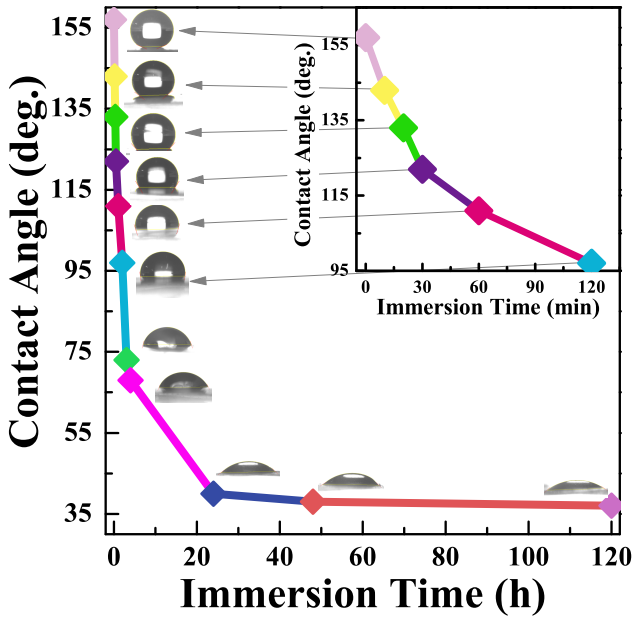

FIG. 12. Plot showing the effect of immersion in water on the contact angle of a plasma-treated FEP sample.

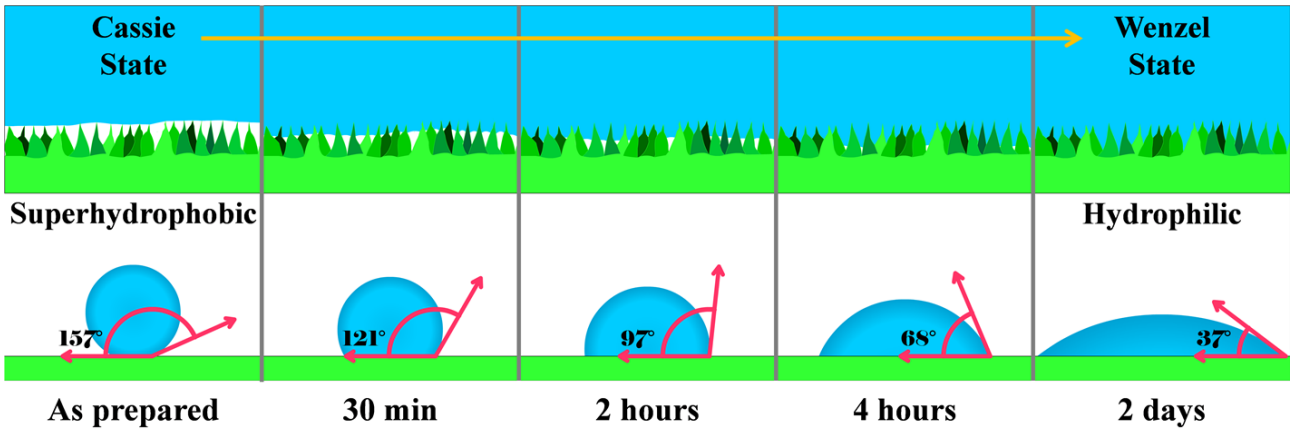

FIG. 13. Schematic representation of the transition from Cassie state to the Wenzel state of the plasma-treated FEP surface as it is immersed in water for the durations 0 s (as prepared), 30 min, 2 h, 4 h and 2 days. The contact angle decreases as the wetting regime shifts from Cassie towards Wenzel state.